Impact of Antenna Geometry on MIMO Communication in Indoor Clustered Channels

Antonio Forenza* and Robert W. Heath Jr.
Wireless Networking and Communications Group, ECE Department
The University of Texas at Austin
1 University Station C0803, Austin, TX 78712-0240 USA
Phone: +1-512-425-1305, {forenza,rheath}@ece.utexas.edu

Introduction

The capacity and error rate performance of MIMO (multiple-input multiple-output) wireless communication systems depends explicitly on the spatial correlation of the channel perceived by the physical layer [1]. Characterization of the spatial correlations - essential for accurately predicting system performance - is challenging due to the interdependence between the propagation environment and the antenna geometry. One generic MIMO channel model that has emerged in a variety of applications of MIMO communication is the clustered channel model. In this model, scatterers are grouped in clusters, experiencing delay and angular spreads. Previous work has focused on evaluating performance in this channel under a uniform linear and circular array assumption. Other array geometries, despite potential implementation advantages, have been neglected.

In this paper we study the impact of different array configurations in indoor propagation environments. We measure the capacity/diversity gain attainable by different array geometries with seven elements and fixed *interelement spacing*. To make the discussion more concrete, we base our simulations on the *IEEE 802.11n* Technical Group (TG) clustered channel model. Our results show that averaged with respect to cluster location, uniform linear arrays often yield the highest capacity/diversity gains. However, in poor scatterer environments and for compact arrays the "Star" configuration provides the best system performance.

Model Description

Consider a broadband communication link with M_t transmit antennas and M_r receive antennas. For simulation purposes, the discrete-time channel is modeled as a matrix impulse response with L matrix taps $\{\mathbf{H}_l\}_{l=0}^{L-1}$. In the correlated Rayleigh fading model [2] each tap is generated independently

$$\mathbf{H}_l = \mathbf{R}_r^{1/2}\mathbf{H}_w\mathbf{R}_t^{1/2} \tag{1}$$

where $\mathbf{H}_w$ is a M_rxM_t matrix of complex Gaussian fading coefficients, and $\mathbf{R}_r$ and $\mathbf{R}_t$ are the spatial covariance matrices at the receiver and transmitter, respectively, expressing the correlation of the receive/transmit signals across the array elements. In this paper we generate $\mathbf{R}_r$ and $\mathbf{R}_t$ for different array configurations according to the indoor clustered channel model. Since the same method is applied at the transmitter and receiver, we will use the notation $\mathbf{R}$ to refer to both the covariance matrices. Likewise, we will use M, instead of M_r or M_t, for the number of array elements. For simplicity we focus on a system with a single tap.

One common modelling technique for indoor propagation environments is the well known Saleh-Valenzuela model [3], which describes multiple propagation paths as channel taps grouped in clusters. An extension to include the effect of the angles of arrival has been proposed in [4]. Each cluster is characterized by a mean angle-of-arrival (AoA) and consists of multi-paths, with AoAs random distributed according to certain probability density function (pdf), modelling the power azimuth spectrum (PAS). The standard deviation of the PAS describes the angular spread (AS) of the cluster. The Saleh-Valenzuela clustered channel model has been adopted by different standardization forums, such as the IEEE 802.11 TGn [5]. Here the PAS is chosen to exhibit Laplacian pdf. Moreover, the channel taps of a given cluster are assumed to experience the same AS and mean AoA as the cluster itself. Therefore we simulate the spatial covariance matrix on a cluster by cluster basis.

0-7803-8302-8/04/$20.00 ©2004 IEEE

Spatial Characteristics of Different Array Configurations

The spatial covariance matrix ($\mathbf{R}$) is computed for different antenna array configurations, employing the 802.11n TGn indoor channel model briefly described above. This model simulates $\mathbf{R}$ through statistical method, for the particular case of uniform linear array (ULA). Since we need to generate $\mathbf{R}$ for different array geometries, we use a discrete model based on statistical distribution of the AoAs of the incoming rays [6]. A large number of rays is simulated in order to converge to the 802.11n channel model (which assumes continuous PAS). Moreover, we consider antenna arrays consisting of dipole elements, with uniform amplitude excitation and no coupling between array elements.

With these assumptions, we can express the spatial correlation matrix for each ray as product of steering-vectors. Simulating P rays per cluster, the covariance matrix of the cluster is derived as

$$\mathbf{R} = \sum_{p=1}^{P} \mathbf{a}(\phi_0 - \phi_p)\ \mathbf{a}^H(\phi_0 - \phi_p) \tag{2}$$

where $\mathbf{a}(\phi)$ is the steering vector for a generic AoA ϕ, ϕ_0 is the mean AoA of the cluster and ϕ_p is the AoA offset with respect to ϕ_0 for the p-th ray. Note that ϕ_p is random variable with Laplacian pdf. This formula substituted in equation (1) provides the MIMO channel matrix used for the simulations described in the next section.

Hereafter we report the expression of the steering vectors at the AoA ϕ for different array geometries, as illustrated in Fig. 1, according to definitions in [7].

- **Uniform Linear Array** (ULA): $\mathbf{a}(\phi) = \left[1, ..., e^{jkd\sin\phi}\right]^T$ with d being the antenna spacing and $k = 2\pi/\lambda$ the wave number.
- **Nonuniformly Spaced Linear Array** (NULA): $\mathbf{a}(\phi) = \left[e^{jkd_1\sin\phi}, ..., e^{jkd_M\sin\phi}\right]^T$ where $d_1, ..., d_M$ are the spacings for the M antennas with respect to the origin of the reference system. We choose the antenna spacings such that the total array aperture coincides with the length of the ULA for a fixed number of elements ($\sum_{i=1}^{M} d_i = Md$). We also assume symmetry with respect to the center of the array as in Fig. 1.
- **Uniform Circular Array** (UCA): $\mathbf{a}(\phi) = \left[e^{jk\rho\cos(\phi-\phi_1)}, ..., e^{jk\rho\cos(\phi-\phi_M)}\right]^T$ with ρ being the radius of the circular array, and ϕ_m the angle of the m-th array element with respect to the reference angle as depicted in Fig. 1.
- **"Hexagon" Array**: $\mathbf{a}(\phi) = \left[1,\ e^{jk\rho\cos(\phi-\phi_1)}, ..., e^{jk\rho\cos(\phi-\phi_6)}\right]^T$
- **"Star" Array**:
  $\mathbf{a}(\phi) = \left[1,\ e^{jkd\cos(\phi-\phi_1)}, ..., e^{jkd\cos(\phi-\phi_3)},\ e^{jk2d\cos(\phi-\phi_4)}, ..., e^{jk2d\cos(\phi-\phi_6)}\right]^T$
  where we designed the star with 3 branches and $M = 7$ array elements.

Results

We analyze the system performance in different propagation conditions and show capacity gain and diversity advantage attainable with the antenna configurations described above. We assume equal power (EP) transmission across different elements and compute the mutual information as [2]

$$C_{EP}(\mathbf{H} = \log_2\left[\det\left(\mathbf{I}_{M_r} + \frac{SNR}{M_t}\,\mathbf{H}\mathbf{H}^H\right)\right] \tag{3}$$

where $\mathbf{H}$ is derived from (1), SNR is the average signal-to-noise ratio, and $\mathbf{I}_{M_r}$ is the identity matrix with dimensions M_rxM_r. To explore the diversity gain due to different array configurations we compute the symbol error rate (SER), *assuming spatial multiplexing*, minimum mean squared error (MMSE) receiver [2] and QPSK modulation. This reflects a typical "high-capacity" approach to communication, but only achieves a fraction of the diversity of space-time codes.

We first show how the system capacity may vary as function of the the mean AoA of the clusters. In Fig. 2 the evolution of the ergodic capacity versus the average SNR is depicted for a single cluster (with $AS = 15^o$) located at broadside (BS) and endfire (EF) directions

with respect to the alignment of the ULA (i.e., $\phi_0 = 0^o$ and $\phi_0 = 90^o$, respectively, as in Fig. 1). For each case 4000 channel realizations are simulated. The normalized element spacing is $d/\lambda = 0.5$. The ULA yields the highest capacity for the BS case. For EF direction the "Star" configuration outperforms the others, whereas the capacity of the ULA drops down dramatically due to the high spatial correlation. Note that in this case NULA provides slightly better capacity than ULA and lower spatial correlation. The "Hexagon" array yields higher spatial correlation (and lower capacity) than the UCA, due to its more compact geometry. In the next results we did not simulate the NULA and "Hexagon" since they provide average system performance similar to the ULA and UCA, respectively.

Now we show the performance of these array configurations in different propagation scenarios. We simulated the channel with 1 and 5 clusters, and values of AS=15^o (low) and AS=40^o (high). We simulated 800 different propagation scenarios, where each cluster mean AoA is uniform distributed in the range $[-\pi,\pi)$, and with 2000 channel realizations each. This gives us an average of the cluster location. The cumulative density function (CDF) of the mutual information is derived from equation (3), for SNR=$10dB$. The Fig. 3 shows that the "Star" configuration gives the highest ergodic and outage capacity for low AS and single cluster scenario. When the channel is characterized by low correlation (i.e., high AS and many clusters) the ULA is the optimal geometry since it contains the most decorrelation, due to the furthest spacing.

We then analyzed the system performance with respect to the antenna parameters. Particularly, we computed the evolution of the ergodic capacity (at SNR= $10dB$) as function of the normalized antenna spacing (d/λ), for different AS and number of clusters. We generated the mean AoA in the range $[-\pi, \pi)$ and the results are shown in Fig. 4. For small spacings the "Star" configuration produces the lowest spatial correlation, yielding the best system performance. At higher element distance the ULA outperforms the other array geometries. The oscillatory behavior of the capacity in Fig. 4 is due to the oscillations of the spatial correlation function from a finite number of rays used to simulate $\mathbf{R}$ [6] or the effect of superposition of multiple clusters [8]. The evolution of the SER is shown in Fig. 5 for d/λ = 1. For low AS, a single cluster and SNR= $15dB$, the ULA yields about $8dB$ diversity gain versus the UCA, and about $2dB$ versus the "Star", due to its higher array aperture. At high AS, with many clusters and at SNR= $15dB$, the ULA provides about $2dB$ array gain. The ULA seems to provide better separability for spatial multiplexing.

Conclusions

We conclude that the "Star" configuration is preferable to the other configurations for MIMO systems characterized by high spatial correlation. This is the case when compact arrays (i.e., small element spacing) are employed, or when the channel exhibits high spatial correlation (i.e., clusters at EF directions, poor scattering environments). On the other hand, when the channel has low correlation, the ULA outperforms the other array geometries. Further investigations are needed to characterize the system performance in more realistic scenarios, with compact configurations and pattern / polarization considerations [9].

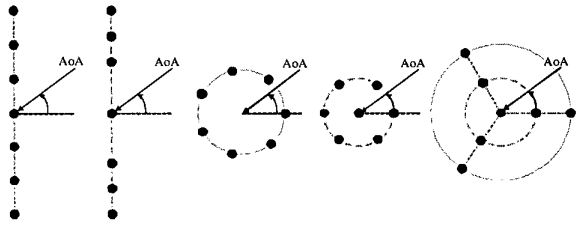

a) ULA b) NULA c) UCA d) Exagon e) Star

Figure 1: Antenna array configurations and reference systems.

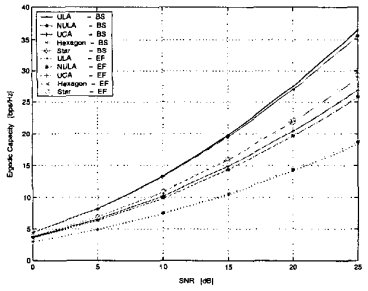

Figure 2: Ergodic Capacity with single cluster at broadside (BS) and endfire (EF) directions, $d/\lambda = 0.5$ and AS= 15°.

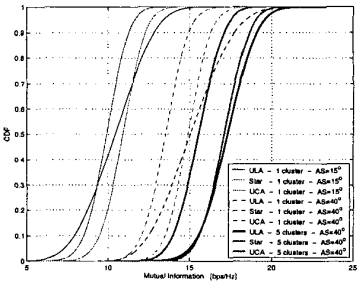

Figure 3: CDF of the mutual information (at SNR=10dB) for different values of angular spread and number of clusters, and $d/\lambda = 0.5$.

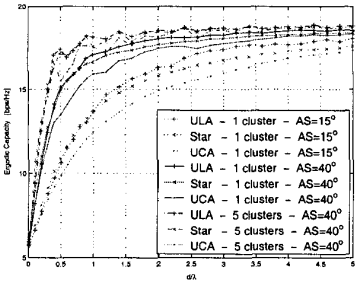

Figure 4: Ergodic capacity as function of d/λ for different array geometries, at SNR=10dB.

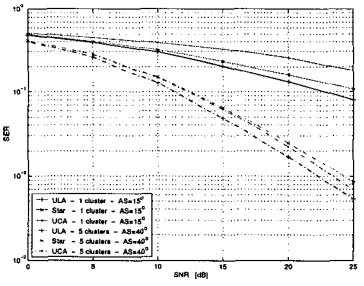

Figure 5: SER in different propagation scenarios for the various array geometries with d/λ=1.

References

[1] D.-S. Shiu, G. J. Foschini, M. J. Gans, and J. M. Kahn, "Fading correlation and its effect on the capacity of multielement antenna systems," *IEEE Trans. Commun.*, vol. 48, no. 3, pp. 502–513, March 2000.

[2] A. Paulraj, R. Nabar, and D. Gore, *Introduction to Space-Time Wireless Communications*, Cabridge University Press, 40 West 20th Street, New York, NY, USA, 2003.

[3] A. A. M. Saleh and R. A. Valenzuela, "A statistical model for indoor multipath propagation," *IEEE JSAC*, vol. SAC-5, no. 2, pp. 128–137, February 1987.

[4] J. W. Wallace and M. A. Jensen, "Statistical characteristics of measured MIMO wireless channel data and comparison to conventional models," *IEEE VTC'01*, vol. 2, pp. 1078–1082, Oct. 2001.

[5] V. Erceg et al., "TGn channel models," IEEE P802.11, 802.11-03/940r2, January 2004.

[6] R. B. Ertel, P. Carderi, K. W. Sowerby, T. S. Rappaport, and J. H. Reed, "Overview of spatial channel models for antenna array communication systems," *IEEE PC*, pp. 10–22, February 1998.

[7] C. A. Balanis, *Antenna Theory: Analysis and Design (second edition)*, Wiley, NY, 1982.

[8] L. Schumacher, K. I. Pedersen, and P.E. Mogensen, "From antenna spacings to theoretical capacities - guidelines for simulating MIMO systems," *PIMRC*, pp. 587–592, Sept. 2002.

[9] L. Dong, H. Ling, and R. W. Heath Jr., "Multiple-input multiple-output wireless communication systems using antenna pattern diversity," *IEEE Globecom'02*, vol. 1, pp. 997–1001, Nov. 2002.